JCTC Journal of Chemical Theory and Computation

Article

pubs.acs.org/JCTC

Computation of the Isotropic Hyperfine Coupling Constant: Efficiency and Insights from a New Approach Based on Wave Function Theory

Emmanuel Giner,*[,†] Lorenzo Tenti,[†] Celestino Angeli,[†] and Nicolas Ferré[‡]

[†]Dipartimento di Scienze Chimiche e Famaceutiche, Universita di Ferrara, Via Fossato di Mortara 17, I-44121 Ferrara, Italy

[‡]Aix-Marseille Univ, CNRS, ICR, Marseille, France

Supporting Information

ABSTRACT: The present paper reports an original computational strategy for the computation of the isotropic hyperfine coupling constants (hcc). The algorithm proposed here is based on an approach recently introduced by some of the authors, namely, the first-order breathing orbital self-consistent field (FOBO-SCF). The approach is an almost parameter-free wave function method capable to accurately treat the spin delocalization together with the spin polarization effects while staying in a restricted formalism and avoiding spin contamination. The efficiency of the method is tested on a series of small radicals, among which four nitroxide radicals and the comparison with high-level *ab initio* methods show very encouraging results. On the basis of these results, the method is then applied to compute the hcc of a challenging system, namely, the DEPMPO-OOH radical in various conformations. The reference values obtained on such a large system allows us to validate a cheap computational method based on density functional theory (DFT). Another interesting feature of the model applied here is that it allows for the rationalization of the results according to a relatively simple scheme based on a two-step mechanism. More precisely, the results are analyzed in terms of two separated contributions: first the spin delocalization and then the spin polarization.

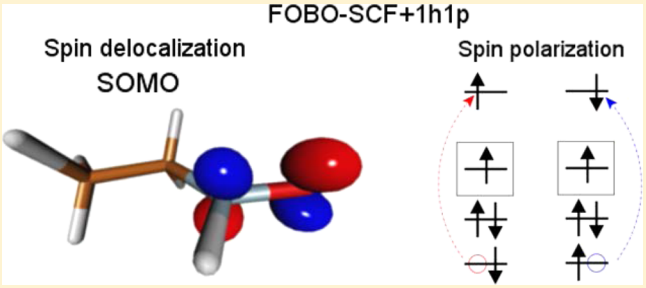

INTRODUCTION

Among the magnetic properties characterizing a paramagnetic molecule (Zeeman interaction, zero-field splitting, etc.), the hyperfine coupling interaction brings essential information regarding the distribution of the unpaired electrons and their chemical environment.[1] Accordingly, the common interpretation of an electron spin resonance (ESR) experiment relies on the use of an effective spin Hamiltonian whose parameters are fitted to reproduce the ESR spectrum. Alternatively, these parameters can be obtained from first-principles calculations.

The quantum-mechanical (QM) determination of accurate isotropic hyperfine coupling constants (hcc) essentially relies on the precise calculation of the electron density at each nucleus with a nonzero magnetic moment (Fermi contact first-order interaction[2]). In the case of organic radicals like nitroxides, the recipe mainly implies three essential ingredients: (i) a basis set with sufficiently decontracted basis functions at the nuclei of interest, e.g., Chipman,[3] EPR-II and EPR-III,[4] and N07D,[5] (ii) a molecular QM method incorporating the most important electronic correlation effects, like the spin delocalization and the spin polarization ones,[6] and (iii) a method that gives access to the calculation of the electron density. These requirements point toward either highly correlated methods like coupled-cluster theory,[7−9] multireference configuration interaction,[10] perturbation theory,[11] or Kohn−Sham DFT based on a suitable exchange-correlation functional.[12−14] In the latter case, the spin polarization is obtained through the unrestricted formalism, resulting sometimes in a spin contamination which sheds doubt on the quality of the computed hcc values.[15] This drawback has been addressed by Rinkevicius and co-workers by means of restricted−unrestricted DFT calculations.[16]

When these three requirements are met, quantitative agreement with experimental ESR spectroscopy results can be expected for isolated, small, and rigid molecules. However, for many cases of interest, e.g., spin-adducts resulting from the trapping of short-lived radical species by a diamagnetic trap like DEPMPO nitrones,[17] other effects need to be taken into account. As a matter of fact, one of the present authors once devised a multiscale approach, combining molecular dynamics investigation of the structural degrees of freedom together with thousands of effective QM/MM calculations.[18,19] This approach has been successfully applied to the interpretation of the experimental DMPO-OOH and DMPO-OH (the DMPO spin-adduct of the superoxide or hydroxyl radicals) ESR spectrum.[20,21] In this approach, one of the key points was the ability of the low-cost DFT PBE0/6-31+G(d) level of theory to

Received: August 22, 2016
Published: January 17, 2017

DOI: 10.1021/acs.jctc.6b00827
J. Chem. Theory Comput. XXXX, XXX, XXX−XXX

reproduce accurate QCISD/Chipman hcc values obtained from a benchmark set of small nitroxides.[19] Since the 6-31+G(d) basis set is not decontracted near the nuclei, the good agreement was necessarily due to error cancellation that was found constant for a wide range of molecular conformations. However, nothing guarantees the full transferability of such a result to each and every nitroxide. Hence, interest for obtaining new reference hcc values for large radicals or even hcc values with a more controlled accuracy is still present.

In that respect, the FOBO-SCF+1h1p method recently developed by some of the authors is promising. Since it was already shown to produce accurate spin densities,[22] its application to the computation of hcc values looks straightforward. Hence, after having recalled briefly some details of the method, we first assess its accuracy by confronting the hcc values computed at the FOBO-SCF+1h1p level of theory to already reported hcc values obtained by state-of-the-art *ab initio* methods,[8,9] namely, quadratic CI with singles and doubles substitutions (QCISD), orbital optimized coupled-cluster with double substitutions (OO-CCD), coupled-cluster with singles and doubles substitutions (CCSD), and its version including the correction from noniterative triple substitutions (CCSD(T)). Then, the method is used to study the dependence of the hcc values with the nitrogen pyramidalization degree of freedom for four small nitroxides radicals, and the results are compared to QCISD level of theory. The very good agreement with QCISD reference values is interpreted in light of the spin delocalization and spin polarization mechanisms. Finally, we apply the FOBO-SCF+1h1p method on the DEPMPO-OOH radical resulting from the trapping of the superoxide radical by the DEPMPO nitrone.[17] The corresponding complex ESR spectrum is usually interpreted using a model spin Hamiltonian featuring couplings with ^{1}H, ^{14}N, and ^{31}P nuclei for different DEPMPO-OOH isomers/conformers in chemical exchange, hence including many parameters whose determination is often ambiguous and takes benefit from computational chemistry calculations. In this context, the theoretical determination of the DEPMPO-OOH hcc values is a challenging task as the dimensions of this system are prohibitive for high-level wave function-based methods as CCSD or QCISD. Nevertheless, our choice of this system was motivated by the importance of this efficient spin trap in the monitoring of biological processes,[17,23−26] like lipid peroxidation inducing DNA or membrane damages. The present study enables us to provide reliable reference hcc values on this realistic system which eventually validate a much cheaper computational approach based on DFT. Once more, the results are analyzed in light of the spin delocalization and spin polarization mechanisms.

THEORY: RECALL OF FOBO-SCF EQUATIONS

General Ideas. The approach proposed here to compute accurate spin densities relies on a very recently introduced method that is based on a two-step mechanism:[22] FOBO-SCF +1h1p. In such an approach, one first introduces the correct spin delocalization by optimizing the singly occupied molecular orbitals (SOMOs) in a restricted formalism with the FOBO-SCF method. Then, the FOBO-SCF determinant is used as a starting point to introduce spin polarization by adding all the one-hole-one-particle (1h1p) determinants in a CI treatment. The resulting wave function, referred here as FOBO-SCF +1h1p, is not affected by spin contamination as it uses a restricted formalism and contains all the determinants required to provide an eigenfunction of $\mathbf{S}^2$. This CI treatment of the 1h1p excitations allows us to take into account the differential orbital relaxation of the α and β spin orbitals, together with a part of the dynamical correlation. As the present work involves only single radical species, we present the equations of FOBO-SCF in the case of a doublet spin state for the sake of clarity.

Notations. The determinant having an "ROHF-like" occupation ($S_z = \frac{1}{2}$) is referred to as $|\Phi_0\rangle$, in which the SOMO is labeled a, the doubly occupied orbitals are labeled i, j, and the virtual orbitals are labeled r, s. According to these notations, the one-hole (1h) determinants are simply

$$|1h_i\rangle = a^{\dagger}_{a,\beta}a_{i,\beta}|\Phi_0\rangle \tag{1}$$

and the one-particle (1p) determinants are

$$|1p_r\rangle = a^{\dagger}_{r,\alpha}a_{a,\alpha}|\Phi_0\rangle \tag{2}$$

Concerning the 1h1p determinants, those who are single excitations with respect to $|\Phi_0\rangle$ can be written as

$$\begin{aligned} |(1h_i1p_r)^{\alpha}\rangle &= a^{\dagger}_{r,\alpha}a_{i,\alpha}|\Phi_0\rangle \\ |(1h_i1p_r)^{\beta}\rangle &= a^{\dagger}_{r,\beta}a_{i,\beta}|\Phi_0\rangle \end{aligned} \tag{3}$$

and those reversing the spin in the SOMO (referred here as spin-flip 1h1p) are simply

$$|1h_i1p_r\rangle = a^{\dagger}_{r,\alpha}a_{a,\alpha}a^{\dagger}_{a,\beta}a_{i,\beta}|\Phi_0\rangle \tag{4}$$

The set of all elements of the density matrix of a given wave function $|\psi\rangle$ is formally referred to with

$$\langle\psi|\rho|\psi\rangle \equiv \{\langle\psi|a^{\dagger}_{n\alpha}a_{m\alpha} + a^{\dagger}_{n\beta}a_{m\beta}|\psi\rangle,\ \forall\ m, n\} \tag{5}$$

and the density matrix of $|\Phi_0\rangle$ is indicated here with ρ^0.

FOBO-SCF Algorithm. As has been shown in a large number of studies,[27−37,41,42] the spin delocalization that appears at a high-level *ab initio* treatment is related to the coefficients acquired by the 1h and 1p determinants when a part of the electronic correlation is introduced. The correlation effect increasing the weights of the 1h and 1p determinants is known as the dynamic charge polarization, which allows for the orbital relaxation of the 1h and 1p determinants.[27,28,34,37,41,42] The dominant effects can be introduced in a CI treatment thanks to the single excitations on top of the 1h and 1p determinants.[27,34,36,37,41,42] The FOBO-SCF optimization procedure here only sketched out (see ref 22 for more details) manages to approximate the natural orbitals of the wave function, which contains the configuration $|\Phi_0\rangle$ and all the important 1h and 1p determinants with proper coefficients. Such a wave function, expressed in intermediate normalization, can be written as

$$|\Phi_0 + 1h + 1p\rangle \equiv |\Phi_0\rangle + \sum_i c_i^{1h}|1h_i\rangle + \sum_r c_r^{1p}|1p_r\rangle \tag{6}$$

and the corresponding one body density matrix is approximated by

$$\begin{aligned} &\langle\Phi_0 + 1h + 1p|\rho|\Phi_0 + 1h + 1p\rangle \\ &\quad\approx \rho^0 + \sum_i \delta\rho(1h_i) + \sum_r \delta\rho(1p_r) \end{aligned} \tag{7}$$

DOI: 10.1021/acs.jctc.6b00827
J. Chem. Theory Comput. XXXX, XXX, XXX−XXX

where the differential density matrices $\delta\rho(1h_i)$ and $\delta\rho(1p_r)$ are defined as

$$\delta\rho(1h_i) \equiv \langle \Phi_0 + c_i^{1h} 1h_i | \rho | \Phi_0 + c_i^{1h} 1h_i \rangle - \rho^0$$
$$\delta\rho(1p_r) \equiv \langle \Phi_0 + c_r^{1p} 1p_r | \rho | \Phi_0 + c_r^{1p} 1p_r \rangle - \rho^0 \quad (8)$$

Thanks to the approximation of eq 7, the coefficients of the $|1h_i\rangle$ and $|1p_r\rangle$ determinants can be determined independently, which drastically reduces the computational cost. Considering a given $|1h_i\rangle$ determinant (or a $|1p_r\rangle$ determinant), this is simply done by diagonalizing the CI matrix within $|\Phi_0\rangle$, $|1h_i\rangle$ ($|1p_r\rangle$) and all determinants $|\mu\rangle$ being single excitations on top of both $|\Phi_0\rangle$ and $|1h_i\rangle$ ($|1p_r\rangle$)

$$|\mu\rangle \equiv \{a^\dagger_{m,\sigma} a_{n,\sigma} |\Phi_0\rangle \text{ or } a_{n,\sigma}|1h_i\rangle \quad \forall\ m, n, \sigma\} \quad (9)$$

This allows for the dominant orbital relaxation effects of $|\Phi_0\rangle$ and $|1h_i\rangle$ ($|1p_r\rangle$). To speed up calculations, an estimation of the importance of the coefficient of the $|1h_i\rangle$ ($|1p_r\rangle$) in the CI wave function is done thanks to the intermediate Hamiltonian theory.[38] In practice, we build the 2×2 dressed matrix

$$\langle K|H^{(\mathrm{int})}_{1h_i}|L\rangle = \langle K|H|L\rangle + \sum_\mu \frac{\langle K|H|\mu\rangle\langle\mu|H|L\rangle}{\langle\Phi_0|H|\Phi_0\rangle - \langle\mu|H|\mu\rangle} \quad (10)$$

where $|K\rangle$ and $|L\rangle$ can be the $|\Phi_0\rangle$ and $|1h_i\rangle$ ($|1p_r\rangle$) determinants. If the $|1h_i\rangle$ ($|1p_r\rangle$) configuration has a coefficient larger than a given threshold η, then the actual CI diagonalization is performed, and the corresponding differential density matrix is computed according to eq 8. When all the possible 1h and 1p determinants have been browsed, the total density matrix is built according to eq 7, and the natural orbitals are used for the next iteration of the FOBO-SCF algorithm.

Modifications to FOBO-SCF Algorithn. Some minor modifications have been brought to the original FOBO-SCF algorithm for the present study.

- When considering the $|\mu\rangle$ in eq 9, we also include all the other determinants needed to have an eigenfunction of S^2. This insures that each step of the FOBO-SCF orbital optimization process deals with pure spin states.
- At the beginning of a given FOBO-SCF iteration, we perform an orbital optimization for the determinant Φ_0 but keeping the SOMO unchanged. This insures to minimize the energy of Φ_0 without changing the SOMO. We have observed that such an optimization step speeds up the CI calculations involved in the FOBO-SCF algorithm. The algorithm is considered to be converged when the difference in energy of the $|\Phi_0\rangle$ determinant between two iterations is lower than 10^{-9} hartree.

NUMERICAL RESULTS AND DISCUSSIONS

Comparison with High-Level *ab Initio* Methods: NH_2, PH_2, NCH_2, and C_2H_3 Radicals. In order to test the accuracy of hcc computed at the FOBO-SCF+1h1p level, we have performed a series of calculations on the NH_2, PH_2, NCH_2 and C_2H_3 radicals for which restricted CCSD(T) (R-CCSD(T)) and unrestricted CCSD(T) (U-CCSD(T)) calculations are available in large basis sets.[8,9] The geometries used for the NH_2, PH_2, and NCH_2 radicals are the equilibrium geometry obtained by Puzzarini et al. at the CBS+CV+fT+fQ level, and the aug-cc-pCVQZ_et4 basis set has been used for all the computations (see ref 9 for details). Concerning the C_2H_3 radical, we used the geometry obtained at the UCCSDT/CBS3 level by Al Derzi et al.,[8] and all calculations have been performed using the cc-pCVTZ, with all *s* functions fully uncontracted for the carbon atoms and the basis set for the hydrogens the cc-pVTZ-t5s-a6.[39] For the sake of comparison, we have performed UHF, OO−CCD, CCSD, and QCISD calculations using an unrestricted formalism (using the Orca program[40]); all the numerical results for hcc concerning the NH_2, PH_2, NCH_2, and C_2H_3 radicals are summarized in Tables 1 and 2 (labels of the atoms used for the vinyl radical are shown in Figure 1).

Table 1. hcc (in Gauss) Computed at Various Levels of Theory for NH_2 and PH_2 Radicals[a]

	NH_2		PH_2	
	H	N	H	P
U-CCSD(T)[b]	−23.73	9.84	−17.36	72.70
OO-CCD	−24.58	10.21	−17.38	72.95
CCSD	−24.78	9.86	−17.23	71.88
QCISD	−25.28	9.85	−17.14	68.39
FOBO-SCF+1h1p	−23.77	8.99	−16.59	83.25
ROHF+1h1p	−24.02	9.66	−16.65	82.70
UHF	−36.17	19.78	−21.04	127.87

[a]See text for details on the geometries and basis sets used. [b]Results from ref 9.

Regarding the FOBO-SCF+1h1p and ROHF+1h1p methods, one can notice two different trends from the results of Tables 1 and 2: for the NH_2 and PH_2 radicals, these two methods give very similar results, whereas for the NCH_2 and C_2H_3 radicals the hcc computed are quite different, especially for the C_2H_3 molecule. The similar behavior found for the NH_2 and PH_2 radicals has to be related to the very small weight of the 1h and 1p determinants observed in the FOBO-SCF calculations, which means that the SOMOs obtained at the ROHF and FOBO-SCF levels are very similar. Also, as planar geometry has been considered for these two molecules, the SOMOs vanishes in the molecular plane, and consequently, the nonvanishing hcc come only from the spin polarization effect. This effect is discussed in more details later in the case of the four nitroxide radicals studied here. Regarding the C_2H_3 radical, the strong difference in performance between the ROHF+1h1p and FOBO-SCF+1h1p methods can be explained by the presence of quite large coefficients (up to 0.1) for some 1h and 1p determinants in the FOBO-SCF calculation, implying substantial differences in the delocalization of the SOMOs obtained at the ROHF and FOBO-SCF levels of theory.

Concerning the accuracy of the FOBO-SCF+1h1p hcc values, one can notice a deviation of 0.84 G (NH_2) and 1.11 G (NCH_2) for the nitrogen atom, with respect to U-CCSD(T), representing a deviation of 9% and 12%, respectively. In the case of the hydrogen hcc, all deviations are below 1 G, which amount to 5% in NH_2 and PH_2, 10% in NCH_2, and 15%, 4%m and 1% for H_3, H_4, and H_5 in C_2H_3, respectively. Regarding the carbon hcc, the deviations are generally smaller: 0.23 and 4.23 G in C_2H_3 representing 3.8% and 3.5% of the R-CCSD(T) reference value, respectively, and 2.67 G in NCH_2, representing 10% of the value obtained at the U-CCSD(T) level of theory. Finally, the FOBO-SCF+1h1p P hcc differs by 10.45 G (14%) from the U-CCSD(T) reference.

The coupled-cluster type methods (QCISD, CCSD, and OO-CCD) produce similar hcc values in the case of NH_2 and PH_2, in very good agreement with the reference U-CCSD(T)

DOI: 10.1021/acs.jctc.6b00827
J. Chem. Theory Comput. XXXX, XXX, XXX−XXX

Table 2. hcc (in Gauss) Computed at Various Levels of Theory for NCH_2 and C_2H_3 Radicals

	NCH_2			C_2H_3				
	N	C	H	C_1	C_2	H_3	H_4	H_5
U-CCSD(T)[a]	8.81	−26.38	77.22					
R-CCSD(T)[b]				−6.50	109.9	13.60	60.00	36.00
OO-CCD	9.77	−29.05	75.88	−7.27	112.97	11.14	54.62	32.8
CCSD	9.10	−29.93	78.11	−8.47	114.38	8.58	56.76	35.61
QCISD	10.58	−35.17	81.50	−13.40	119.61	5.36	59.51	38.64
FOBO-SCF+1h1p	7.70	−29.05	84.76	−6.73	105.67	15.55	57.98	36.19
ROHF+1h1p	8.15	−24.07	55.75	−2.72	122.62	13.45	40.44	23.98
UHF	24.30	−75.92	82.49	−41.46	169.17	−13.05	67.05	46.67
Chipman basis set								
OO-CCD	10.27	−31.18	73.91	−8.27	119.41	10.97	56.20	94.97
CCSD	9.59	−32.04	75.94	−9.53	120.90	7.72	58.39	36.62
QCISD	11.32	−37.61	79.03	−14.89	126.58	4.26	61.29	39.81
FOBO-SCF+1h1p	7.44	−30.34	83.94	−6.49	110.16	12.25	61.52	36.33
ROHF+1h1p	8.00	−24.67	53.83	−2.97	128.74	13.16	41.30	24.47
UHF	24.67	−67.17	84.51		173.86	−13.87	68.52	47.81
Complete basis set extrapolation								
CBS[a]	9.11	−27.56	78.69					
CBS[b]				−6.00	110.00	14.60	60.10	36.40

[a]Results from ref 9. [b]Results from ref 8.

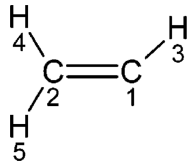

Figure 1. Labels of the atoms of the vinyl radical.

values. However, NCH_2 and C_2H_3 hcc values significantly depend on the level of theory. For instance, in the case of C_2H_3, only OO-CCD manages to reproduce hcc values close to the R-CCSD(T) ones. These differences can be explained by the T_1 diagnostic in the QCISD and CCSD calculations. For NH_2 and PH_2, it is small ($\approx 9 \times 10^{-3}$). The largest amplitudes come from double excitations, at variance with NCH_2 and C_2H_3 for which it is quite large ($\approx 4 \times 10^{-2}$), and the largest amplitudes come from single excitations. Nevertheless, in the particular case of C_2H_3, one observes that the hcc values globally improve going from QCISD to CCSD and to OO-CCSD. Such a trend would suggest that the orbital optimization is particularly important in this system, eventually explaining the large T_1 diagnostic observed in our calculations and also in previous works.[8]

The quality of the basis set is known to be important to obtain reliable hcc values. Accordingly, we performed calculations using the double-ζ plus polarization basis set designed by Chipman[44] for the NCH_2 and C_2H_3 radicals; the results are reported in Tables 1 and 2, where we also report the results obtained by Puzzarini et al.[9] and Al Derzi et al.[8] from complete basis set extrapolations (CBS). From these data, one can observe that the results obtained using the Chipman basis set are quite similar to those obtained using a larger basis set whatever the method, confirming the quality of the Chipman basis set. Also, one can notice that the results obtained in the latter basis set at FOBO-SCF+1h1p compares quite well with the CBS results, especially for the challenging case of the C_2H_3 radical.

In all, the present systematic study demonstrates that the FOBO-SCF+1h1p method provides hcc values in quite good agreement with the R-CCSD(T) or U-CCSD(T) reference values. Maximum deviations of 14% have been obtained in the case of phosophorus hcc; however, the deviation is usually smaller. The FOBO-SCF+1h1p method looks more accurate than QCISD, CCSD, or OO-CCSD when a large T_1 diagnostic is found, as for the case of the C_2H_3 radical for instance. Also, regarding the coupled-cluster like methods not including triple excitations, one can observe that when the QCISD, CCSD, and OO-CCD give very similar values, the results obtained with these three methods are in close agreement with U-CCSD(T), whereas when a large discrepancy is observed, a large T_1 diagnostic is also found.

Case of Nitroxides: Computational Details and Reference Values. The systems studied here consist of a series of four nitroxide single radicals, which are schematically represented in Figure 2: dihydronitroxide (DHNO), dimethyl nitroxide (DMNO), methyl nitroxide (MNO), and ethyl nitroxide (ENO).

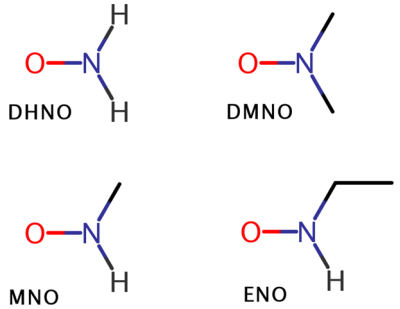

Figure 2. Schematic representation of the nitroxides models studied here.

All calculations have been performed within the double-ζ plus polarization basis set designed by Chipman.[44] The geometries have been optimized at the unrestricted QCISD level using the Gaussian09 software.[45] The DFT calculations and UHF and ROHF calculations have been performed using the Gamess(US) software,[46] and all CI calculations together

DOI: 10.1021/acs.jctc.6b00827
J. Chem. Theory Comput. XXXX, XXX, XXX−XXX

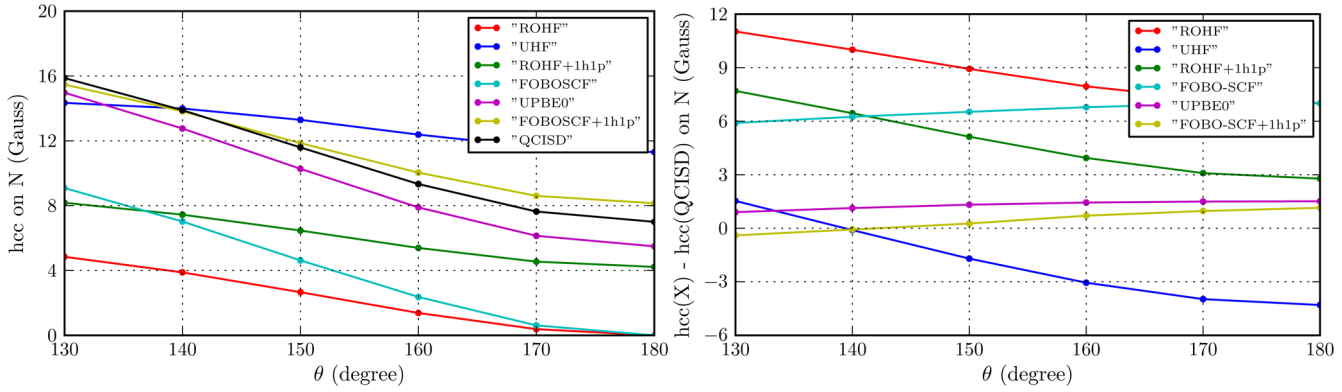

Figure 3. Isotropic hyperfine constant on the nitrogen nucleus of the DHNO compound as a function of θ (eq 11) and corresponding errors with respect to the QCISD values, using various computational strategies.

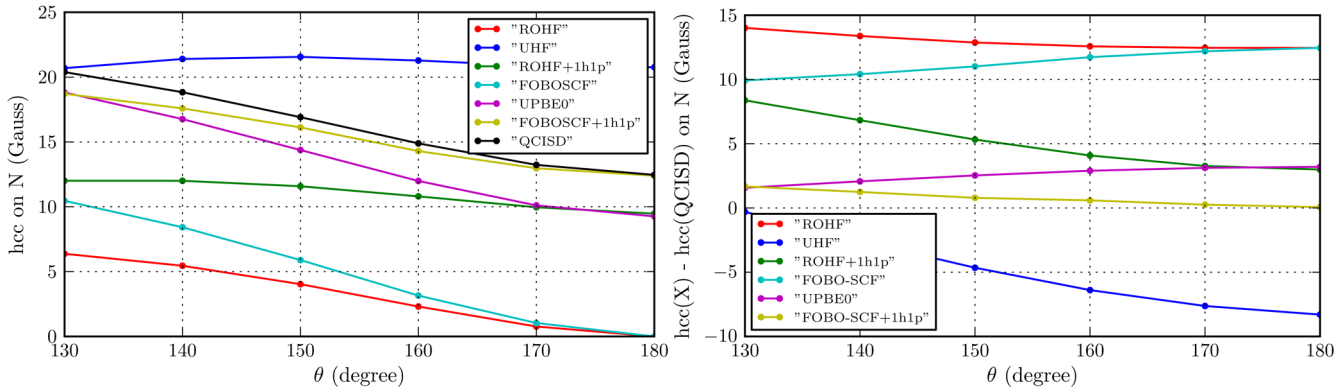

Figure 4. Isotropic hyperfine constant on the nitrogen nucleus of the DMNO compound as a function of θ (eq 11) and corresponding errors with respect to the QCISD values, using various computational strategies.

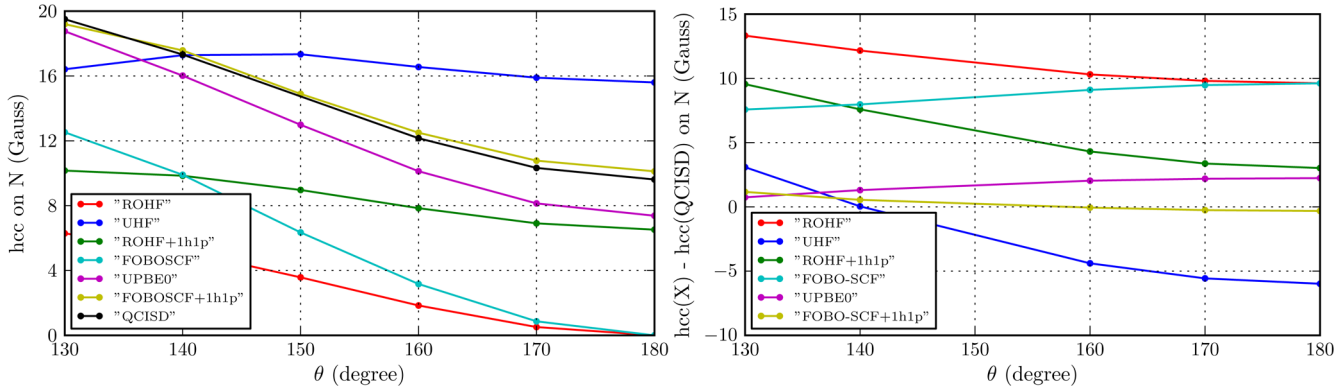

Figure 5. Isotropic hyperfine constant on the nitrogen nucleus of the ENO compound as a function of θ (see eq 11) and corresponding errors with respect to the QCISD values, using various computational strategies.

with the FOBO-SCF calculations have been performed using the Quantum Package.[47] The CCSD and OO-CCD calculations have been performed with the Orca package.[40] The threshold η introduced for the estimation of the 1h and 1p coefficients in the FOBO-SCF procedure has been fixed to 10^{-4}. For all systems, we investigate the hcc dependency with the geometrical parameter representing the nitrogen out-of-plane degree of freedom. This is quantified by the angle θ derived from the improper dihedral angle ∠XNYO (X, Y = H, C), and θ is simply defined (in degree) as

$$\theta = 180 - \angle\mathrm{XNYO} \tag{11}$$

In order to produce accurate reference hcc values for nitroxides, we have performed calculations at the QCISD, CCSD, and OO-CCD levels of theory on the smallest nitroxide studied here (DHNO) using the six geometries related to the pyramidalization degree of freedom of the nitrogen center (results reported in the SI), complemented with hcc calculations for the two extreme values of θ (i.e., θ = 180° and θ = 130°) in MNO, ENO, and DMNO (results reported in the SI). All these three methods lead to very similar hcc values, whatever the geometry or the nitroxide. Together with our results regarding NH_2, PH_2, NCH_2, and C_2H_3, it is reasonable to think that these values can be considered as accurate. Consequently, we select the cheapest QCISD

DOI: 10.1021/acs.jctc.6b00827
J. Chem. Theory Comput. XXXX, XXX, XXX−XXX

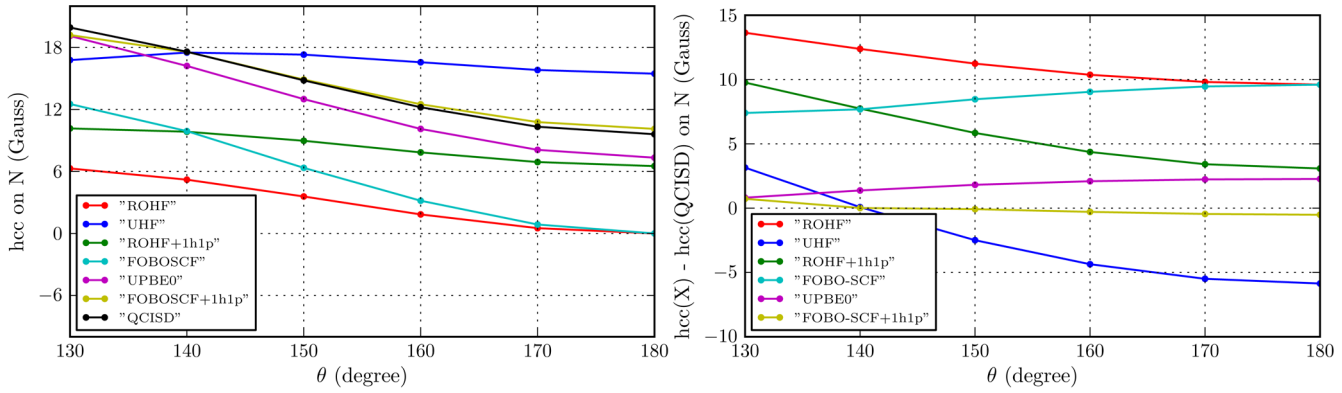

Figure 6. Isotropic hyperfine constant on the nitrogen nucleus of the MNO compound as a function of θ (eq 11) and corresponding errors with respect to the QCISD values, using various computational strategies.

method to provide reference values in the following study of the dependence of the nitrogen hcc with its pyramidalization.

Results for the Four Nitroxides. We report in Figures 3, 4, 5, and 6 the hcc computed on the nitrogen atom at various levels of theory using wave function methods, together with the corresponding errors with respect to the QCISD values for the DHNO, DMNO, ENO, and MNO radicals, respectively. Calculations of the hcc using the unrestricted PBE0[48] approach (UPBE0) are also reported, as such methodology has become the standard way to compute the hcc.[14]

From these figures, one can observe some general trends. Regarding the single Slater determinant models in a restricted formalism (ROHF, FOBO-SCF), they all fail to give non-vanishing hcc at the planar geometry even if they reproduce qualitatively the global shape of the hcc obtained at the QCISD level when the geometry is distorted from planarity. Nevertheless, the absolute error at the ROHF level is very large (more than 10 G, typically), and the FOBO-SCF determinant manages to significantly reduce this error when the geometry is nonplanar (by roughly 5 G when θ = 130°). Considering now the unrestricted approaches used here, the hcc obtained at the UHF level is not able to reproduce the global shape of the reference values, even if the absolute error is lower than the ROHF and FOBO-SCF ones. The values of the hcc obtained at the UPBE0 level are in good agreement with the reference values, and one can notice that this method performs much better at the distorted geometry than at the planar one, where it systematically underestimates the hcc by about 2 or 3 G. Finally, when considering the restricted models with a multideterminantal wave function (namely, ROHF+1h1p and FOBO-SCF+1h1p), one clearly sees that the CI treatment of the 1h1p determinants improves the quality of the hcc with respect to the single Slater determinant description (namely, ROHF and FOBO-SCF). Nevertheless, there is a major difference between the ROHF+1h1p and FOBO-SCF+1h1p curves as the former shows an absolute error varying between 3 and 10 G when moving from the planar geometry to the distorted one, whereas the latter has an error ranging between 0.06 and 1.67 G. Among all methods used here, the FOBO-SCF+1h1p model is the most accurate and gives a quantitative approximation of the hcc obtained at the QCISD level. Also, one can notice the following: (a) The FOBO-SCF model and its FOBO-SCF+1h1p variant are uniquely defined for a given system and a basis set. (b) These models are nonempirical as they deal with purely *ab initio* treatments. (c) The typical cost is much cheaper than the QCISD model as the size of the largest CI space to be diagonalized in the FOBO-SCF model scales as $6 \times n_{docc} \times n_{virt}$, which is 2 orders of magnitude less than the scaling of $n_{docc}^2 \times n_{virt}^2$ intrinsic to the QCISD model. The last point is important as the bottleneck of any optimization step involved in a CI or CC formalism is the memory required to store the CI coefficients or CC amplitudes, which means that the FOBO-SCF algorithm can treat much larger systems than QCISD as is shown on the DEPMPO-OOH radical but keep a comparable accuracy.

Starting from these values, the following sections are dedicated to the analysis of the results obtained at the various levels of theory used here, and attention is focused on two mechanisms: spin delocalization and spin polarization.

Interpretation of Results: Role of Spin Delocalization and Spin Polarization. *Contribution of Spin Delocalization.* Let us first focus our attention on the importance of the spin delocalization mechanism in the computation of hcc. To this aim, here we only analyze the restricted approaches that use a single Slater determinant (ROHF, FOBO-SCF), in which the spin density is nothing but the square of the SOMO. Accordingly, hcc is directly proportional to the square of the SOMO evaluated at the nitrogen nucleus. From Figures 3, 4, 5, and 6, it clearly appears that the hcc obtained using these approaches is vanishing when the species have a planar geometry (θ = 180°), whereas they grow considerably as one distorts the geometry to reach their maximum values for θ = 130°. This behavior can be qualitatively understood using simple chemical arguments. At the planar geometry, the nitrogen atom is sp^2 hybridized which implies that the SOMO is a pure π^* orbital involving only the p_z atomic orbitals of the nitrogen and oxygen atoms, where the z axis is orthogonal to the XNYO plane. As the p functions vanish in the XNYO plane, the SOMO vanishes on the nitrogen nucleus, explaining the vanishing of the hcc on the nitrogen atom. On the other hand, when the geometry is distorted, the nitrogen atom is sp^3 hybridized, which means that the SOMO will acquire an s component on the nitrogen. Consequently, the more sp^3 hybridized is the nitrogen atom, the larger is the s component from the nitrogen atom in the SOMO, and so the larger is hcc on the nitrogen atom. This mechanism suggests that the s component of the spin density increases as one distorts the geometry, which is precisely what has been observed by computing the s component of the Mulliken spin density (Figure 7) on the nitrogen atom (N-MSD) represented in Figure 8.

DOI: 10.1021/acs.jctc.6b00827
J. Chem. Theory Comput. XXXX, XXX, XXX−XXX

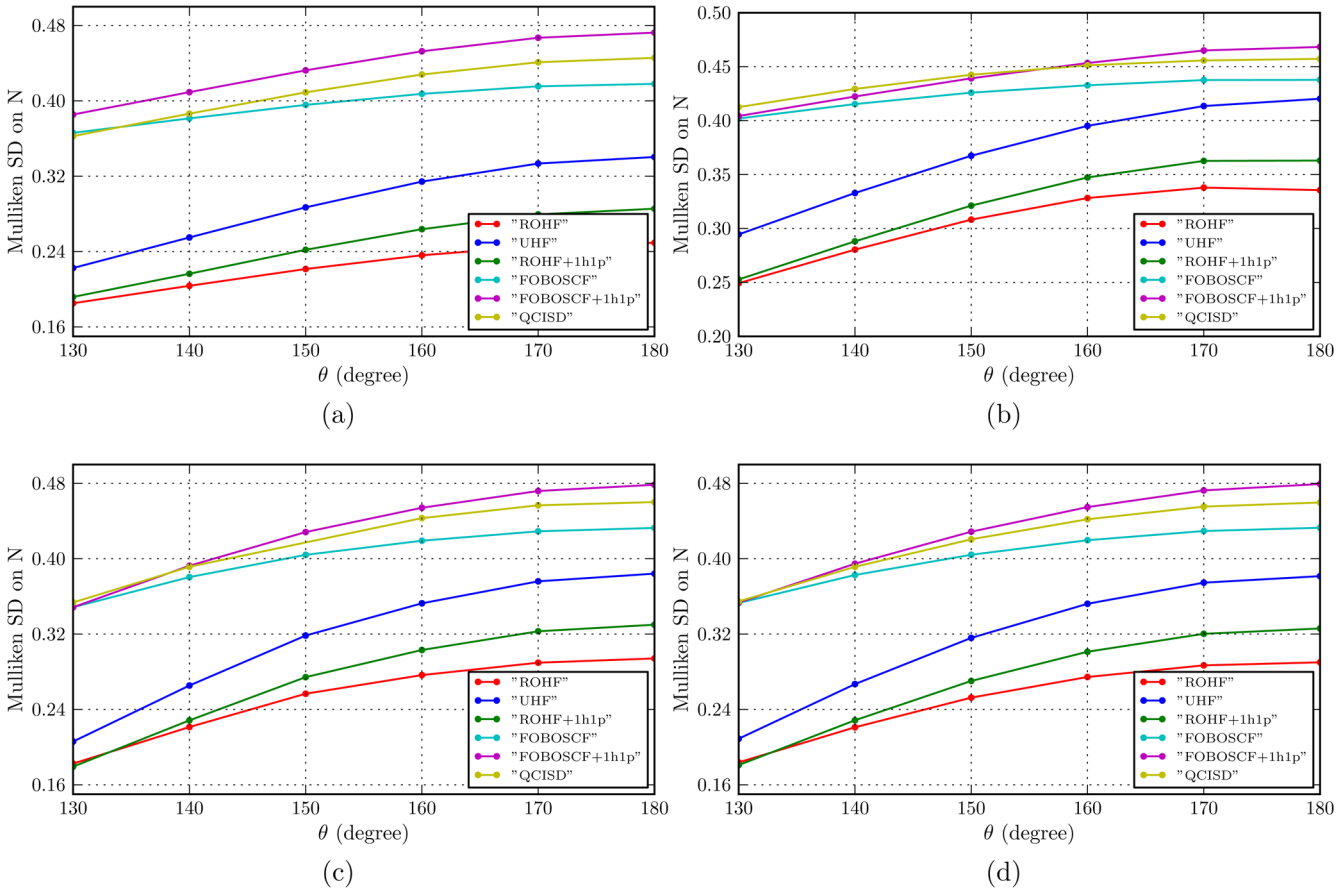

Figure 7. Mulliken spin density on the nitrogen atom of the DHNO (a), DMNO (b), ENO (c), and DMNO (d) compounds, using various computational strategies.

Except for these qualitative discussions, the difference between the hcc obtained at the ROHF and FOBO-SCF levels is striking: as one distorts the geometry, the increase in hcc is much larger using the FOBO-SCF approach than using the standard mean-field approximation. Also, one can observe that the nonparallelism error with respect to the QCISD curves is considerably lowered when going from the ROHF to the FOBO-SCF approaches. One can link these improvements to the values of the N-MSD: the ROHF systematically underestimates the delocalization of the unpaired electron on the nitrogen atom, whereas the FOBO-SCF algorithm gives a value of the N-MSD much closer to the one provided by the QCISD method (Figure 7). This implies that the FOBO-SCF optimization procedure manages to correctly reproduce the spin delocalization of the unpaired electron within the NO moiety. The analysis of our calculations have shown that, starting from the ROHF orbitals, the most important contribution to the spin delocalization brought by the FOBO-SCF algorithm is given by rotations between two orbitals: The SOMO that can be thought as a π^* orbital within the NO moiety, and a doubly occupied molecular orbital that has been identified as the corresponding π orbital. This mixing between the π and π^* orbitals is directly linked to the delocalization of the unpaired electron, which in the CI language leads to a large coefficient of a single excitation of a β electron from the π to the π^* orbital. The excessive localization of the unpaired electron (here on the oxygen atom) is a characteristic of the mean field approach and has been observed in other systems, both organic[41,42] and inorganic.[32,34,36,37,43]

Contribution of Spin Polarization. Our attention is now focused on the second part of the mechanisms at work in the correct determination of the spin density: spin polarization. This effect expresses the differential response of the closed shell α and β electrons to the presence of unpaired electrons. Chipman has published a very complete and pedagogical review[49] of the importance of the spin polarization effects in the context of the computation of hcc, and the inclusion of this mechanism is known to be compulsory to have a quantitative description of these quantities.[14] In the context of organic diradicals, Kollmar et al. have highlighted the role of the spin polarization mechanism,[50,51] which leads to a singlet ground state rather than a triplet ground state as it would be expected according to Hund's rule.

The spin polarization cannot be taken into account using a single CSF in a restricted formalism, as at this level of treatment no differential effects are included for the closed shell α and β electrons. The most standard way to introduce the spin polarization is to use a single Slater determinant in an unrestricted formalism, both in wave function theory (UHF) or density functional theory (unrestricted Kohn–Sham, UKS). In these formalisms, part of the differential response of the α and β electrons is taken into account thanks to the use of different spatial parts for the α and β spin orbitals. One of the advantages of such techniques relies in their cheap computational cost, with the drawback of the spin contamination. Recently,[22] some of the present authors proposed an alternative approach which uses a CI treatment in a restricted formalism. In such an approach, we use a specific class of CI excitations, [illegible] (see Notations),

DOI: 10.1021/acs.jctc.6b00827
J. Chem. Theory Comput. XXXX, XXX, XXX−XXX

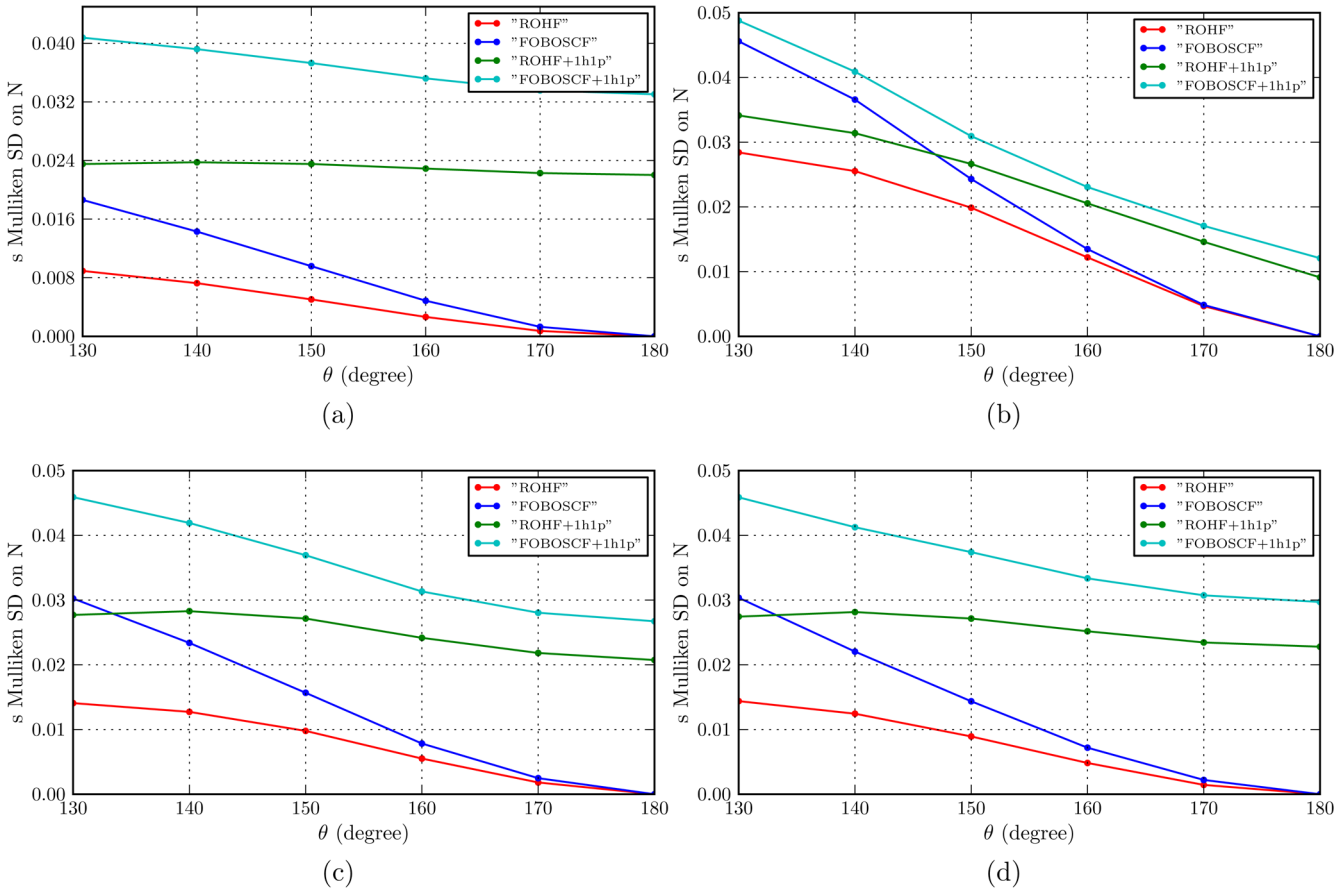

Figure 8. The *s* component of the Mulliken spin density on the nitrogen atom of the DHNO (a), DMNO (b), ENO (c), and DMNO (d) compounds, using various computational strategies.

which introduces two different but connected physical effects: the dominant part of the differential orbital relaxation of the α and β orbitals and part of the dynamical correlation between the unpaired α electron and the β electrons. These two effects are introduced thanks to two types of excitations: The differential orbital optimization is introduced by the 1h1p single excitations on top of $|\Phi_0\rangle$ (eq 3), and the dynamical correlation effect is treated with the spin-flip 1h1p (eq 4), which are double excitations on top of $|\Phi_0\rangle$. The inclusion of both types of excitations allows us to have an eigenfunction of $\mathbf{S}^2$, thus avoiding the spin contamination problems of the unrestricted approaches.

To better understand the importance of the spin polarization in the computation of hcc, we focus our attention on the unrestricted approaches (UHF and UKS) and the restricted approaches that introduces the 1h1p excitations (ROHF+1h1p and FOBO-SCF+1h1p). Looking at the corresponding hcc results, it is noteworthy that all the methods including spin polarization give nonvanishing values for hcc at planar geometries (θ = 180°). This means that the hcc obtained at this specific geometry comes only from the spin polarization mechanism: due to the presence of an unpaired α electron in the π^* orbital, the 1*s* and 2*s* orbitals are different for the α and β electrons, which leads to a nonvanishing spin density on the nucleus. From a CI point of view, this means that the coefficient of a given single excitation depends on whether one excites an α or a β electron. This can be qualitatively understood using single reference perturbation theory—assuming the Møller–Plesset zeroth order Hamiltonian.[52] Consequently, using the Brillouin–Levy–Berthier relation,[53,54] the first-order coefficients of the single excitations 1h1p are

$$c_{ir}^{\alpha(1)} \equiv \frac{\langle \mathrm{ROHF}|H|(1\mathrm{h}_i 1\mathrm{p}_r)^{\alpha}\rangle}{\epsilon_i - \epsilon_r} = -c_{ir}^{\beta(1)} \quad (12)$$

where ϵ_i and ϵ_r are eigenvalues of the Fock-like operator. This simple relation implies that the optimal α spin orbitals are different from the optimal β spin orbitals and that the spin restricted formalism gives a set of doubly occupied MOs, which is a compromise between the request of the α electrons and that of the β electrons (eq 12, the coefficients for the α and β single excitations are equal in absolute value and they have opposite signs). As at the planar geometry, hcc occurs exclusively from the spin polarization mechanism, a[illegible]ne would be tempted to separate the contribution of the [illegible]cc in terms of the spin polarization of the 1*s* and 2*s* orbitals of the nitrogen atom. This can be easily done by performing a series of CI treatment: all 1h1p excitations from the nitrogen 1*s* orbital (which is easily identifiable) introduce the *core spin polarization*, and all the other 1h1p excitations introduce the *valence spin polarization*, which can be understood as the spin polarization of the 2*s* orbitals. These calculations have been performed on all species studied here at the planar geometry using the FOBO-SCF orbitals, and the results are summarized in Table 3. From Table 3, one clearly sees that the core spin polarization always leads to a negative spin density on the nucleus of the nitrogen, whether the valence spin polarization leads invariably to a positive spin density to the same nucleus.

DOI: 10.1021/acs.jctc.6b00827
J. Chem. Theory Comput. XXXX, XXX, XXX–XXX

Table 3. hcc (in Gauss) on Nitrogen Atom Computed at Planar Geometry for DHNO, MNO, DMNO, and ENO Compounds at Various Computational Levels[a]

method	hcc (DHNO)	hcc (MNO)	hcc (ENO)	hcc (DMNO)
FOBO-SCF+1h1p(core)	−10.03	−11.01	−10.81	−12.29
FOBO-SCF+1h1p(valence)	18.42	21.11	20.73	24.60
sum(core + valence)	8.40	10.10	9.92	12.31
FOBO-SCF+1h1p(full)	8.27	10.11	9.93	12.39

[a]See text for details.

Such results imply that the spin polarization of the core and valence electrons follow different trends: the core β electrons tend to get closer to the nucleus, whether the valence β electrons move away from the nucleus, with the α electrons doing the opposite. Also, the spin polarization coming from the core and valence electrons has the same order of magnitude in absolute value, even if the contribution of the valence is found to be roughly twice as large. This means that the actual spin density obtained at the nucleus results from the quasi-compensation of two large quantities of opposite signs. Last but not least, if one sums the spin density obtained from the two independent calculations (core and valence spin polarization), one obtains a very good approximation of the total spin density obtained by the diagonalization of all 1h1p excitations (core and valence spin polarization treated together). This means that the spin polarization coming from the core and valence region are almost uncoupled, suggesting that one could treat separately the core and valence electrons. We emphasize that such differential spin polarization effects between the core and valence electrons seem to be quite general as the same trends have been observed for the spin density on the CH_3 radical and the nitrogen atom (results reported in Table 4). From these results, one can nevertheless

Table 4. Spin Density (in Gauss) at Nucleus of Nitrogen Atom and Carbon Atom of CH_3 Radical at Experimental Equilibrium Geometry Computed at Various Computational Levels[a]

method	N	CH_3
FOBO-SCF+1h1p(core)	−60.33	−44.10
FOBO-SCF+1h1p(valence)	62.09	68.82
sum(core + valence)	1.76	24.72
FOBO-SCF+1h1p(full)	5.04	25.32

[a]See text for details.

notice that the magnitude of the spin polarization mechanism together with the coupling between the core and valence spin polarization are much larger for these two systems with respect to all the nitroxydes studied here.

Except for these general considerations, the accuracy of the methods introducing the spin polarization are qualitatively different. Regarding the UHF method, it is clear that it totally fails to reproduce even the general trends of the dependence of hcc on the improper dihedral angle, unlike the UPBE0 methods, which provide a relatively small error (between 1 and 3 G according to the system and the geometry). From a qualitative point of view, it is interesting to observe that ROHF +1h1p and FOBO-SCF+1h1p follow roughly the same trends, even if ROHF+1h1p systematically strongly underestimates the hcc, whereas the FOBO-SCF+1h1p provides a quantitative description of them. The only difference between ROHF+1h1p and FOBO-SCF+1h1p is the set of MOs on which the CI of the 1h1p is performed, which means that the orbitals play a fundamental role in the spin polarization at the nucleus, in particular, the SOMO, which acounts for the spin delocalization. As mentioned previously, the main difference between the ROHF and FOBO-SCF determinants is that the latter gives a much larger spin density on the nitrogen atom, suggesting that a larger spin density in the valence of the nitrogen atom implies a larger spin polarization and, consequently, a larger hcc. This was also suggested by Improta et al.[14] and recalls the relation obtained by Karplus−Fraenkel for the hcc on the ^{13}C in organic radicals.[55]

Application to DEPMPO-OOH Radical. Having established the reliability of the FOBO-SCF+1h1p method, we hereafter report an application to a real-life nitroxide radical formed by the trapping of the hydroperoxyl radical by the DEPMPO nitrone, namely, the DEPMPO-OOH nitroxide, which is schematically represented in Figure 9. Even if the

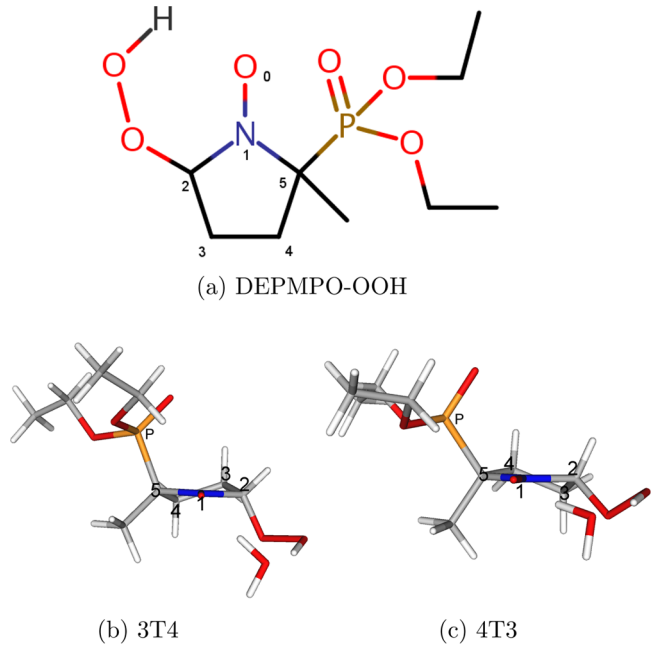

(a) DEPMPO-OOH

(b) 3T4 (c) 4T3

Figure 9. Schematic representation of the DEPMPO-OOH radical (a) and of the two 3T4 (b) and 4T3 (c) geometries used in this study.

DEPMPO-OOH ESR signal is complex, it is dominated by the hcc at the phosphorus nucleus,[26] and therefore, we focus on this quantity. In order to avoid the unlikely geometry constraint in which an intramolecular hydrogen bond would take place between the nitroxide and OOH moieties, we have introduced an explicit water molecule in our model. The basis set used for the ROHF, FOBO-SCF, and FOBO-SCF+1h1p calculations is the cc-pVDZ basis set, except for the four carbon atoms and the nitrogen and oxygen atoms composing the pyrroline-oxide cycle (atoms 0, 1, 2, 3, 4, and 5 in Figure 9) together with the phosphorus atom, for which the aug-cc-pvDZ has been chosen in order to better treat the charge polarization induced by the charge fluctuation of the spin delocalization. Unfortunately, the phosphorus atom is not parametrized in the Chipman basis set; hence, we have replaced all the *s* functions of the P aug-cc-pVDZ basis set by the *s* functions of the aug-cc-pCVTZ in a fully uncontracted way. The resulting all-electron calculations

DOI: 10.1021/acs.jctc.6b00827
J. Chem. Theory Comput. XXXX, XXX, XXX−XXX

Table 5. DEPMPO-OOH Phosphorus Mulliken Spin Density (SD, in |e|) and hcc (in Gauss) at Various Levels of Theory

	$^3T_4$		$^4T_3$	
method	hcc	SD ($\times 10^{-2}$)	hcc	SD ($\times 10^{-2}$)
FOBO-SCF	31.31	1.59	20.78	1.20
ROHF	23.26	1.07	15.92	0.84
FOBO-SCF+1h1p	52.72	2.98	35.85	2.34
ROHF+1h1p	39.26	2.12	27.37	1.68
RO-PBE0/6-31G*	40.33	2.30	28.17	1.69
RO-B3LYP/6-31G*	41.93	2.36	29.44	1.74
UPBE0/6-31G*	51.00	3.06	35.90	2.14
UB3LYP/6-31G*	50.98	2.94	36.03	2.07
RO-PBE0/aug-cc-pCVDZ	42.23	3.06	29.20	2.53
RO-B3LYP/aug-cc-pCVDZ	44.04	3.22	30.64	2.74
UPBE0/aug-cc-pCVDZ	53.58	4.50	37.34	3.97
UB3LYP/aug-cc-pCVDZ	53.70	4.46	37.59	3.94

consider the 153 DEPMPO-OOH electrons using 461 basis functions, leading to 436 molecular orbitals as pure spherical harmonics are used.

The selected DEPMPO-OOH geometries correspond to the two possible "twist" configurations of the N-pyrroline cycle, i.e., two different orientations of the carbon centers 3 and 4 with respect to the 5-membered ring mean plane (see Figure 9 for labels). According to the Cremer and Pople general definition of the ring puckering coordinates,[56] one can label these two geometries as $^3T_4$ and $^4T_3$ (see Figure 9 and SI for explicit Cartesian coordinates). The $^3T_4$ and $^4T_3$ geometries have been optimized at the unrestricted B3LYP level using the 6-31G* basis set. In Table 5, we report for both geometries the P hcc values together with their corresponding Mulliken spin densities, as computed at various computational levels including both wave function theory and DFT.

Several trends can be observed from the results in Table 5. First, the FOBO-SCF method systematically increases the P spin density and hcc values with respect to the ROHF determinant. While the P spin density remains relatively small (between 1 and 2×10^{-2}|e|), the FOBO-SCF approach induces a significant increase of 49% ($^3T_4$) and 43% ($^4T_3$) with respect to the ROHF values. With the same trend being observed for the hcc values (+35% and +64% for the $^3T_4$ and $^4T_3$ geometries, respectively), we conclude that the increase in spin delocalization obtained by the FOBO-SCF algorithm involves a component on the *s* orbitals located on the phosphorus center. By adding the spin polarization with the CI treatment of the 1h1p configurations, the hcc values increase considerably, but the ROHF+1h1p value remains far off the FOBO-SCF+1h1p one. Actually, only the FOBO-SCF+1h1p is able to produce a P hcc value in agreement with the experimentally reported value (about 50 G[17]). Now comparing the hcc values computed for the two geometries of the 5-membered ring, the FOBO-SCF+1h1p method gives the largest difference, about 17 G. This is expected owing to the quasi-axial orientation of the C−P bond in the $^3T_4$ conformer allowing a strong spin delocalization. Conversely, the C−P bond is quasi-equatorial in the $^4T_3$ conformer, strongly reducing the spin delocalization.

Coming to the DFT approach, it is remarkable to observe that both the UPBE0 and UB3LYP in conjunction with the modest 6-31G(d,p) basis set give results that are in quite good agreement with the FOBO-SCF+1h1p calculations, regardless of the DEPMPO-OOH geometry. More precisely, an underestimation of about 1.5 G is observed for the $^3T_4$ conformer, deviating by less than 5% from the FOBO-SCF+1h1p value, whereas an almost perfect agreement is obtained in the case of 4T3. Also, the DFT results depend weakly on the basis set as the same models performed in the aug-cc-pCVDZ slightly overestimates hcc by only 1 G. These latter results show that the addition of tight *s* functions weakly influences the accuracy of hcc using DFT models, even if it might be counterintuitive. Finally, having in mind the quite good results obtained using the UPBE0 model for the four nitroxides studied here, the previous study of the DMPO-OOH and DMPO-OH radicals by Houriez et al.[20,21] and the results obtained for the DEPMPO-OOH radical, one can be tempted to conclude that the UPBE0/6-31G* model is quite well suited for computing hcc in systems involving nitrones and nitroxides. Nevertheless, more studies are to be performed in order to further confirm the reliability of this cheap DFT model.

SUMMARY AND CONCLUSION

In this work, we have investigated the problem of the electronic part of the calculation of the hyperfine coupling constants using a method very recently introduced by some of us, FOBO-SCF +1h1p,[22] with the aim of studying a series of radicals of increasing complexity. First, the accuracy of the method has been tested on a series of four small radicals including the challenging case of the vinyl radical for which high-level *ab initio* theory such as CCSD(T) in large basis sets are available.[8,9] Then, the attention has been focused on a series of four small nitroxides for which the dependency of the nitrogen hcc value on the out-of-plane degree of freedom of the NO moiety has been studied, [illegible]pulsory to correctly reproduce the experimental values.[18,19] [illegible]des the FOBO-SCF+1h1p accuracy, special attention has been paid to the physical/chemical interpretation of the results in terms of a two-step mechanism: spin delocalization and spin polarization. Having established the accuracy and robustness of the FOBO-SCF+1h1p, this method has been applied to the computation of the phosphorus hcc in a realistic nitroxide spin adduct of the hydroperoxide radical, namely, DEPMPO-OOH, in order to provide new reference P hcc values, the dimensions of this system making prohibitive standard coupled-cluster type calculations. Thanks to these reference values obtained with the FOBO-SCF+1h1p, we were able to validate the use of certain popular hybrid exchange-correlation functionals in DFT methods. Nevertheless, in light of the spin delocalization and spin polarization mechanisms, this agreement might be attributed to fortitious error cancellation. For now, we summarize the main insights obtained from

DOI: 10.1021/acs.jctc.6b00827
J. Chem. Theory Comput. XXXX, XXX, XXX−XXX

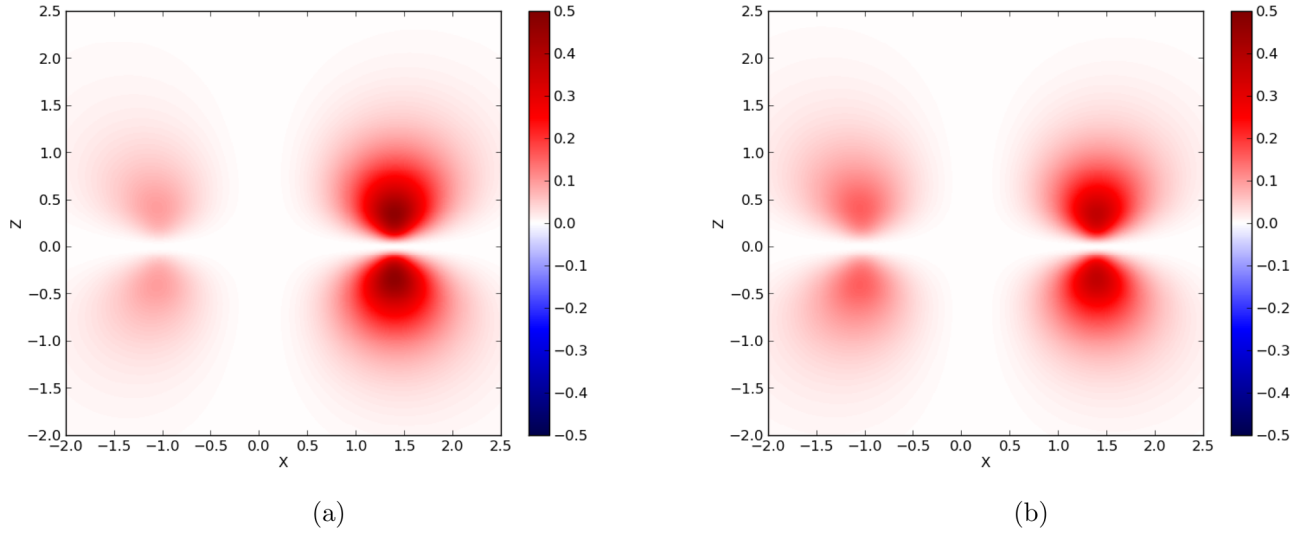

Figure 10. Spin density map of the DHNO compound within the XZ plane ($Y = 0$) at the ROHF level (a) and FOBO-SCF level (b). The molecule lies in the XY plane, and the NO axis corresponds to the X axis.

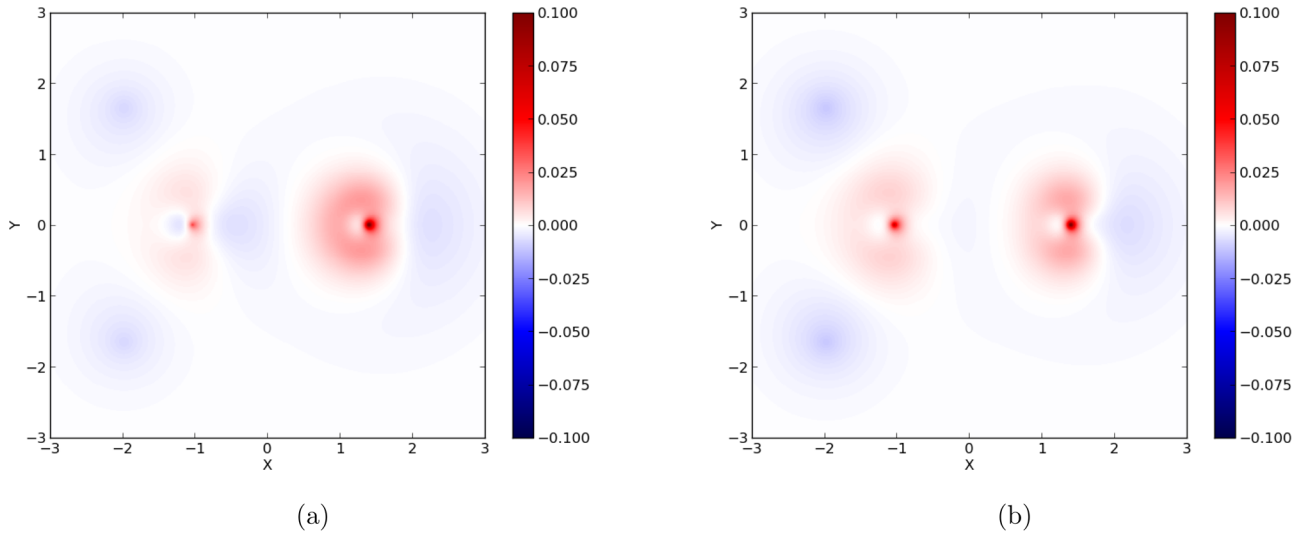

Figure 11. Spin density map of the DHNO compound within the XY plane (Z = 0) at the ROHF+1h1p level (a) and FOBO-SCF+1h1p level (b). The molecule lies in the XY plane, and the NO axis corresponds to the X axis.

the interpretation of the results obtained at the FOBO-SCF +1h1p level.

The main ingredients to compute an accurate spin density can be thought as the following:

1. The accurate description of the spin density in the valence is related to the delocalization of the unpaired electron within the NO moiety, which can be accurately represented by a correctly delocalized SOMO.
2. The spin polarization mechanism depends on the level of delocalization of the SOMO: if the SOMO is correctly delocalized, one can recover an accurate spin density, both in the valence and in the core region, thanks to the proper treatment of spin polarization.

In the context of the hcc on the nitrogen atom, we have shown that the quality of the results of a given method is strongly related to its ability to provide a correct determination of the total spin density on the same atom. This quantity can be thought of as coming from two effects that strongly depends on the level of treatment of the electronic correlation: the amount of delocalization of the SOMO on the nitrogen atom and the additional contribution coming from the spin polarization of the electrons involved in the bondings of the nitrogen. The ROHF method systematically underestimates the delocalization of the SOMO on the nitrogen atom, whereas the FOBO-SCF manages to increase such delocalization, as is illustrated in the case of the DHNO compound at planar geometry in Figure 10. Adding the spin polarization treatment thanks to 1h1p, ROHF+1h1p systematically underestimates the spin density on the nitrogen atom, whereas a quantitative approximation of the QCISD spin density is obtained with the FOBO-SCF+1h1p method. Regarding the spin density at the nucleus at planar geometry, it comes directly from the polarization of the 1s and 2s orbitals, whose contributions have been found to be of opposite signs and weakly coupled. At the same geometry, the total spin density on the nitrogen's nucleus has been found to be an increasing function of the total amount of spin on the nitrogen atom, which explains why ROHF+1h1p underestimates the hcc, whereas FOBO-SCF+1h1p gives a much larger value, in close agreement to the QCISD method. This is

DOI: 10.1021/acs.jctc.6b00827
J. Chem. Theory Comput. XXXX, XXX, XXX−XXX

illustrated in Figure 11 with the DHNO compound: from this figure, it is clear that the spin density on the nitrogen nucleus is no longer vanishing in the XY plane when [illegible] is included and that it is larger using FOBO-SCF+1h1p th[illegible]ROHF+1h1p.

As one distorts the geometry, the nitrogen atom passes from sp^2 to sp^3 hybridization, which brings an *s* component to the SOMO. Therefore, the correct description of the spin delocalization of the SOMO brings a direct contribution to the hcc, and the larger the SOMO on the nitrogen atom i[illegible] larger the hcc on it is. This explains why [illegible] increases as [illegible] distorts the geometry and also why [illegible] gives larger hcc than ROHF at a given distorted [illegible]metry.

To conclude, the main messages of this work are that it is possible to achieve accuracy in the computation of such a subtle quantity as hcc thanks to FOBO-SCF+1h1p, which is a nonempirical method having a reasonable computational cost and which deals with pure *ab initio* elements. Last but not least, this method also allows the understanding of the results for the spin density as coming from two distinct effects, the spin delocalization and spin polarization. These aspects highlight that it is possible to provide interpretable models for the qualitative understanding of rigorous and accurate results, which should be the main goal of quantum chemistry.

■ ASSOCIATED CONTENT

Supporting Information

The Supporting Information is available free of charge on the ACS Publications website at DOI: 10.1021/acs.jctc.6b00827.

Additional *ab initio* calculations on the DHNO, DMNO, ENO, and MNO radicals aiming at establishing the reliability of the hcc computed at the QCISD level of theory. OO−CCD and CCSD calculations have been performed at various geometries and compared to the hcc obtained at the QCISD level of theory, showing an almost perfect agreement. Also, we also report the two geometries used in this work for the study of the DEPMPO-OOH radical. (PDF)

■ AUTHOR INFORMATION

Corresponding Author

*E-mail: gnrmnl@unife.it.

ORCID

Emmanuel Giner: 0000-0002-6206-1103

Nicolas Ferré: 0000-0002-5583-8834

Notes

The authors declare no competing financial interest.

■ REFERENCES

(1) Rieger, P. H. *Electron Spin Resonance: Analysis and Interpretation*; RSC Publishing, 2007.

(2) Kaupp, M.; Bühl, M.; Vladimir, G. *Calculation of NMR and EPR Parameters. Theory and Applications*; Wiley-VCH Verlag GmbH & Co. KGaA, 2004.

(3) Chipman, D. M. Gaussian basis sets for calculation of spin densities in first-row atoms. *Theor. Chim. Acta.* **1989**, *76*, 73−84.

(4) Barone, V. Structure, Magnetic Properties and Reactivities of Open-Shell Species from Density Functional and Self-Consistent Hybrid Methods. In *Recent Advances in Density Functional Methods*; World Scientific, Singapore, 1995; Vol *1*, pp 287−334.

(5) Barone, V.; Cimino, P. Accurate and feasible computations of structural and magnetic properties of large free radicals: the PBE0/N07D model. *Chem. Phys. Lett.* **2008**, *454*, 139−143.

(6) Chipman, B. The spin polarization model for hyperfine coupling constants. *Theor. Chim. Acta* **1992**, *82*, 93−115.

(7) Verma, P.; Perera, A.; Morales, J. A. Massively parallel implementations of coupled-cluster methods for electron spin resonance spectra. I. Isotropic hyperfine coupling tensors in large radicals. *J. Chem. Phys.* **2013**, *139* (17), 174103.

(8) Al Derzi, A. R.; Fau, S.; Bartlett, R. J. Benchmark study of isotropic hyperfine coupling constants for hydrogen: influence of geometry, correlation method, and basis set. *J. Phys. Chem. A* **2003**, *107*, 6656−6667.

(9) Puzzarini, C.; Barone, V. Toward spectroscopic accuracy for open-shell systems: molecular structure andhyperfine coupling constants of H_2CN, H_2CP, NH_2, and PH_2 as test cases. *J. Chem. Phys.* **2010**, *133*, 184301.

(10) Engels, B. Ab Initio Post-Hartree-Fock Calculations of Hyperfine Coupling Tensors and Their Comparison with DFT Approaches. In *Calculation of NMR and EPR Parameters*; Wiley-VCH, 2004; pp 463−482.

(11) Shiozaki, T.; Yanai, T. Hyperfine coupling constants from internally contracted multireference perturbation theory. *J. Chem. Theory Comput.* **2016**, *12* (9), 4347−4351.

(12) Munzarová, M.; Kaupp, M. A critical validation of density functional and coupled-cluster approaches for the calculation of EPR hyperfine coupling constants in transition metal complexes. *J. Phys. Chem. A* **1999**, *103* (48), 9966−9983.

(13) Munzarová, M. DFT calculations of EPR hyperfine coupling tensors. In *Calculation of NMR and EPR parameters*, first ed.; Kaupp, M.; Bühl, M.; Malkin, V. G.Wiley-VCH, 2004; pp 463−482.

(14) Improta, R.; Barone, V. Interplay of electronic, environmental, and vibrational effects in determining the hyperfine coupling constants of organic free radicals. *Chem. Rev.* **2004**, *104* (3), 1231−1254.

(15) Hedegård, E. D.; Kongsted, J.; Sauer, S. P. A. Validating and analyzing EPR hyperfine coupling constants with density functional theory. *J. Chem. Theory Comput.* **2013**, *9* (5), 2380−2388.

(16) Rinkevicius, Z.; Telyatnyk, L.; Vahtras, O.; Ågren, H. Density functional theory for hyperfine coupling constants with the restricted-unrestricted approach. *J. Chem. Phys.* **2004**, *121* (16), 7614−7623.

(17) Frejaville, C.; Karoui, H.; Tuccio, B.; Le Moigne, F.; Culcasi, M.; Pietri, S.; Lauricella, R.; Tordo, P. 5-(diethoxyphosphoryl)-5-methyl-l-pyrrolinne- oxide: a new efficient phosphorylated nitrone for the in vitro and in vivo spin trapping of oxygen-centered radicals. *J. Med. Chem.* **1995**, *38* (2), 258−265.

(18) Houriez, C.; Ferré, N.; Masella, M.; Siri, D. Prediction of nitroxide hyperfine coupling constants in solution from combined nanosecond scale simulations and quantum computations. *J. Chem. Phys.* **2008**, *128*, 244504.

(19) Houriez, C.; Ferré, N.; Siri, D.; Masella, M. Further insights into the incidence of structural fluctuations and environmental effects on the theoretical computations of hyperfine coupling constants of nitroxides in aqueous solution. *J. Phys. Chem. B* **2009**, *113* (45), 15047−15056.

(20) Houriez, C.; Ferré, N.; Siri, D.; Tordo, P.; Masella, M. Structure and spectromagnetic properties of the superoxide radical adduct of the DMPO in water: elucidation by theoretical investigations. *J. Phys. Chem. B* **2010**, *114* (42), 13616.

(21) Houriez, C.; Ferré, N.; Siri, D.; Tordo, P.; Masella, M. Assessing the accuracy of a QM/MM//MD combined protocol to compute spectromagnetic properties of polyfunctional nitroxides in solution. *Theor. Chem. Acc.* **2012**, *131* (6), 1240−1244.

(22) Giner, R.; Angeli, C. Spin density and orbital optimization in open shell systems: a rational and computationally efficient proposal. *J. Chem. Phys.* **2016**, *144* (10), 104104.

(23) Davies, J. L. Recent Developments in EPR-Spin Trapping. In *Electron Paramagnetic Resonance*; Gilbert, B. C., Davies, M. J., Murphy, D. M., Eds.; RSC Publishing, 2002; Vol *18*, pp 47−73.

(24) Inanami, O.; Yamamori, T.; Takahashi, T. A.; Nagahata, H.; Kuwabara, M. ESR detection of intraphagosomal superoxide in polymorphonuclear leukocytes using 5-(diethoxyphosphoryl)-5-methyl-1-pyrroline-N-oxide. *Free Radical Res.* **2001**, *34*, 81.

DOI: 10.1021/acs.jctc.6b00827
J. Chem. Theory Comput. XXXX, XXX, XXX−XXX

(25) Clement, J. L.; Finet, J. P.; Frejaville, C.; Tordo, P. Deuterated analogues of the free radical trap DEPMPO: synthesis and EPR studies. *Org. Biomol. Chem.* **2003**, *1*, 1591.
(26) Karoui, H.; Chalier, F.; Finet, J. P.; Tordo, P. DEPMPO: an efficient tool for the coupled ESR-spin trapping of alkylperoxyl radicals in water. *Org. Biomol. Chem.* **2011**, *9*, 2473.
(27) Janssen, G. J. M.; Nieuwpoort, W. C. Band gap in NiO: a cluster study. *Phys. Rev. B: Condens. Matter Mater. Phys.* **1988**, *38*, 3449−3458.
(28) van Oosten, A. B.; Broer, R.; Nieuwpoort, W. C. Heisenberg exchange enhancement by orbital relaxation in cuprate compounds. *Chem. Phys. Lett.* **1996**, *257*, 207−212.
(29) Calzado, C. J.; Sanz, J. F.; Malrieu, J. P. Accurate ab initio determination of magnetic interactions and hopping integrals in $La_{2-x}Sr_xCuO_4$ systems. *J. Chem. Phys.* **2000**, *112*, 5158−5167.
(30) de Graaf, C.; Sousa, C.; de P. R. Moreira, I.; Illas, F. Multiconfigurational perturbation theory: an effcient tool to predict magnetic coupling parameters in biradicals, molecular complexes, and ionic insulators. *J. Phys. Chem. A* **2001**, *105*, 11371−11378.
(31) Calzado, C. J.; Cabrero, J.; Malrieu, J. P.; Caballol, R. Analysis of the magnetic coupling in binuclear complexes. I. Physics of the coupling. *J. Chem. Phys.* **2002**, *116*, 2728−2747.
(32) Cabrero, J.; Calzado, C. J.; Maynau, D.; Caballol, R.; Malrieu, J. P. Metal ligand delocalization in magnetic orbitals of binuclear complexes. *J. Phys. Chem. A* **2002**, *106*, 8146−8155.
(33) Broer, R.; Hozoi, L.; Nieuwpoort, W. C. Non-orthogonal approaches to the study of magnetic interactions. *Mol. Phys.* **2003**, *101*, 233−240.
(34) Calzado, C. J.; Angeli, C.; Taratiel, D.; Caballol, R.; Malrieu, J. P. Analysis of the magnetic coupling in binuclear systems. III. The role of the ligand to metal charge transfer excitations revisited. *J. Chem. Phys.* **2009**, *131*, 044327.
(35) Vancoillie, S.; Pierloot, K. Multiconfigurational g tensor calculations as a probe for the covalency of the copper-ligand bonds in copper(II) complexes: $[CuCl_4]^{2-}$, $[Cu(NH_3)_4]^{2+}$, and plastocyanin. *J. Phys. Chem. A* **2008**, *112*, 4011−4019.
(36) Caffarel, M.; Giner, E.; Scemama, A.; Ramírez-Solís, A. Spin density distribution in open shell transition metal systems: a comparative post Hartree Fock, density functional theory, and quantum Monte Carlo study of the CuCl2 molecule. *J. Chem. Theory Comput.* **2014**, *10*, 5286−5296.
(37) Giner, E.; Angeli, C. Metal-ligand delocalization and spin density in the $CuCl_2$ and $[CuCl_4]^{2-}$ molecules: some insights from wave function theory. *J. Chem. Phys.* **2015**, *143*, 124305.
(38) Malrieu, J. P.; Durand, P.; Daudey, J. P. Intermediate Hamiltonians as a new class of effective Hamiltonians. *J. Phys. A: Math. Gen.* **1985**, *18*, 809.
(39) Fau, S.; Bartlett, R. J. Gaussian Basis Sets for Highly Accurate Calculations of Isotropic Hyperfine Coupling Constants at Hydrogen. *J. Phys. Chem. A* **2003**, *107*, 6648−6655.
(40) Neese, F. *The ORCA Program System*; Wiley Interdisciplinary Reviews: Computational Molecular Science; **2012**, Vol. *2*, pp 1759−0884.
(41) Suaud, N.; Ruamps, R.; Guihéry, N.; Malrieu, J. P. A strategy to determine appropriate active orbitals and accurate magnetic couplings in organic magnetic systems. *J. Chem. Theory Comput.* **2012**, *8*, 4127−4137.
(42) Suaud, N.; Ruamps, R.; Malrieu, J. P.; Guihéry, N. Singly occupied MOs in mono- and diradical conjugated hydrocarbons: comparison between variational singlereference, π-fully correlated and Hückel descriptions. *J. Phys. Chem. A* **2014**, *118*, 5876−5884.
(43) Spivak, M.; Angeli, C.; Calzado, C. J.; de Graaf, C. Improving the calculation of magnetic coupling constants in MRPT methods. *J. Comput. Chem.* **2014**, *35*, 1665−1671.
(44) Chipman, D. M. Gaussian basis sets for calculation of spin densities in first-row atoms. *Theor. Chim. Acta* **1989**, *76*, 73−84.
(45) Frisch, M. J.; Trucks, G. W.; Schlegel, H. B.; Scuseria, G. E.; Robb, M. A.; Cheeseman, J. R.; Zakrzewski, V. G.; Montgomery, J. A., Jr.; Stratmann, R. E.; Burant, J. C.; Dapprich, S.; Millam, J. M.; Daniels, A. D.; Kudin, K. N.; Strain, M. C.; Farkas, O.; Tomasi, J.; Barone, V.; Cossi, M.; Cammi, R.; Mennucci, B.; Pomelli, C.; Adamo, C.; Clifford, S.; Ochterski, J.; Petersson, G. A.; Ayala, P. Y.; Cui, Q.; Morokuma, K.; Salvador, P.; Dannenberg, J. J.; Malick, D. K.; Rabuck, A. D.; Raghavachari, K.; Foresman, J. B.; Cioslowski, J.; Ortiz, J. V.; Baboul, A. G.; Stefanov, B. B.; Liu, G.; Liashenko, A.; Piskorz, P.; Komaromi, I.; Gomperts, R.; Martin, R. L.; Fox, D. J.; Keith, T.; Al-Laham, M. A.; Peng, C. Y.; Nanayakkara, A.; Challacombe, M.; Gill, P. M. W.; Johnson, B.; Chen, W.; Wong, M. W.; Andres, J. L.; Gonzalez, C.; Head-Gordon, M.; Replogle, E. S.; Pople, J. A. *Gaussian 09*, Revision D.01; Gaussian, Inc.: Wallingford, CT, 2001.
(46) Gordon, M. S.; Schmidt, M. W. Advances in Electronic Structure Theory: GAMESS, A Decade Later. In *Theory and Applications of Computational Chemistry: The First Forty Years*; Dykstra, C. E., Frenking, G., Kim, K. S., Scuseria, G. E., Eds.; Elsevier: Amsterdam, 2005; Vol. *1*, pp 1167−1189.
(47) Scemama, A.; Giner, E.; Applencourt, T.; David, G.; Caffarel, M. Quantum Package v0.6, 2015.
(48) Adamo, C.; Barone, V. Toward reliable density functional methods without adjustable parameters: the PBE0 model. *J. Chem. Phys.* **1999**, *110*, 6158−6170.
(49) Chipman, D. M. The spin polarization model for hyperfine coupling constants. *Theor. Chim. Acta* **1992**, *82*, 93−115.
(50) Kollmar, H.; Staemmler, V. A theoretical study of the structure of cyclobutadiene. *J. Am. Chem. Soc.* **1977**, *99* (11), 3583−3587.
(51) Kollmar, H.; Staemmler, V. Violation of hund's rule by spin polarization in molecules. *Theor. Chim. Acta* **1978**, *48*, 223−239.
(52) Møller, C.; Plesset, M. *Phys. Rev.* **1934**, *46*, 618.
(53) Brillouin, L. Le champ self-consistent pour des électrons liés la supraconductibilité. *J. Phys. Radium* **1933**, *4*, 333−361.
(54) Levy, B.; Berthier, G. Generalized Brillouin theorem for multiconfigurational SCF theories. *Int. J. Quantum Chem.* **1968**, *2*, 307−319.
(55) Karplus, M.; Fraenkel, G. K. Theoretical interpretation of carbon-13 hyperfine interactions in electron spin resonance spectra. *J. Chem. Phys.* **1961**, *35*, 1312−1323.
(56) Cremer, D.; Pople, J. A. *J. Am. Chem. Soc.* **1975**, *97* (6), 1354−1358.

DOI: 10.1021/acs.jctc.6b00827
J. Chem. Theory Comput. XXXX, XXX, XXX−XXX